

B.Tech Project Report

**Long Term Voltage Stability Analysis for Integrated
TD systems**

Kritika Agrawal : 2021EE1664
Tarun Gupta: 2021EE30482

Supervised by: Professor Ankit Singhal

May 8, 2025

Contents

1	Abstract	2
2	Aim	2
3	Introduction	2
4	Limitation	2
5	Solution	3
6	System Overview	3
7	CPF	3
	7.1 Literature review	3
	7.2 Methodology	4
	7.2.1 Results of CPF	6
	7.2.2 Inference	7
	7.3 Lumped Distribution System	8
	7.3.1 Methodology	8
	7.3.2 Derivation	8
	7.3.3 Results	9
	7.3.4 Inferences	10
	7.4 Addition of Renewable Energy Source	10
	7.4.1 Different Cases	11
	7.4.2 Inferences	14
8	Jacobian Determinant Analysis	15
	8.1 Determinant of Jacobian using CPF	15
9	Voltage Stability Index (VSI)	17
	9.1 Introduction	17
	9.2 Methodology	17
	9.3 Results	18
	9.4 Inference	18
10	Transmission Distribution Distinguishing Index	19
	10.1 Introduction	19
	10.2 Result	19
11	Bus Participation Factor	19
	11.1 V-Q sensitivity Analysis	19
	11.2 Modes	20
	11.3 Bus Participation Factor	20
	11.4 Conclusion	21
12	References	22

1 Abstract

Traditional voltage stability assessment methods have analyzed transmission (T-VSA) and distribution (D-VSA) systems independently, relying on oversimplified assumptions such as aggregated transmission-level loads and fixed substation voltages in distribution networks. These approaches fail to capture critical interactions between the two subsystems, leading to inaccurate load margin predictions. This study investigates integrated transmission-distribution voltage stability assessment (TD-VSA) using a co-simulation framework that couples detailed 3-phase unbalanced distribution models with transmission systems. We demonstrate that distribution networks—particularly under high penetration of distributed energy resources (DERs) and load unbalance—can become the limiting factor for overall system loadability, a phenomenon overlooked in conventional T-VSA. Through PV curve analysis and net-load unbalance (NLU) metrics, we quantify how distribution system losses, voltage dependencies (ZIP loads), and DER controls (volt-VAR) impact the voltage stability margin (VSM). Our results highlight the necessity of TD co-simulation for accurate VSM assessment and provide a practical methodology to bridge the gap between transmission and distribution planning

2 Aim

To study loadability limits using integrated Transmission-Distribution (TD-VSA) analysis using Voltage Stability Indices (VSI), Bus Participation Factors (BPF), and Transmission-Distribution Distinguishing Index (TDDI), with a comparative evaluation against traditional Transmission Voltage Stability Assessment (T-VSA) method.

To propose equivalent feeder impedance methods as a compromise between accuracy and computational efficiency for large-scale studies.

3 Introduction

Transmission Voltage Stability Assessment (T-VSA) is a crucial method for evaluating the ability of a power transmission system to maintain stable voltage levels across all buses under varying load conditions. Voltage stability is a key aspect of power system reliability, referring to the system’s capability to sustain acceptable voltage magnitudes at all buses—points where power is either injected by generators or consumed by loads. A stable voltage profile ensures that the system can deliver power efficiently without voltage collapses, which could lead to blackouts or operational disruptions. T-VSA specifically analyzes the transmission network’s ability to handle changes in load demand and disturbances, such as faults or line outages, while maintaining voltages within acceptable limits. During normal operation, T-VSA assesses whether the system can sustain expected load levels without significant voltage drops or deviations. In post-disturbance scenarios, it evaluates how quickly and effectively the system can recover to stable voltage levels after events like faults, generator trips, or sudden changes in load. The method is particularly important for identifying the loadability limits of the transmission system, or the maximum load the system can handle without entering an unstable voltage condition.

Considering the recent evolution of the power system, the assumptions made in several methods of power system analysis should be re-evaluated. Increasing proliferation of DERs and other smart controllable loads are making the distribution system behavior more uncertain. This uncertainty resulting from the distributed controllable loads and DERs is forcing the inclusion of the distribution system along with the transmission system for more accurate analysis of the power systems. One influence of the high DER penetrations is a change in the load composition observed over the recent years.

4 Limitation

Traditional methods for analyzing voltage stability in power systems often simplify the way loads are modeled. Instead of considering how power is distributed to each bus or area, all the loads are combined into one large, single load. While this makes the calculations faster, it misses the details of how power is actually used across the network. This can lead to overly optimistic estimates of how much load the system can handle before it becomes unstable. A more detailed approach that looks at both transmission and distribution levels is needed for a clearer and more accurate understanding of system stability.

5 Solution

As T-VSA has limitations when used independently, an integrated Transmission-Distribution Voltage Stability Assessment (TD-VSA) is necessary for an accurate analysis of voltage stability. TD-VSA takes into account:

1. The interaction between transmission and distribution systems.
2. The variation of substation voltage is based on transmission conditions.
3. How distribution systems might limit the loadability of the transmission system, and vice versa.
4. By comparing lumped vs. detailed models, we can estimate how and when systems should be modeled. Lumped models overestimate Lambdamax .

This integrated approach provides a more accurate picture of the overall system's voltage stability and loadability

6 System Overview

Transmission System: IEEE 9 Bus system

Distribution System: 4 bus Radial system

For most of the analysis, the distribution system was attached to bus 5 of the transmission system. In the IEEE 9 bus system, bus 5 consumes real power near 90 MW. In the initial distribution system, each consumed 9MW of power, so a total of 10 distribution systems were attached in parallel. The transmission system has a base voltage of 345kV and a distribution system of 7.2kV. So a transformer is connected between them.

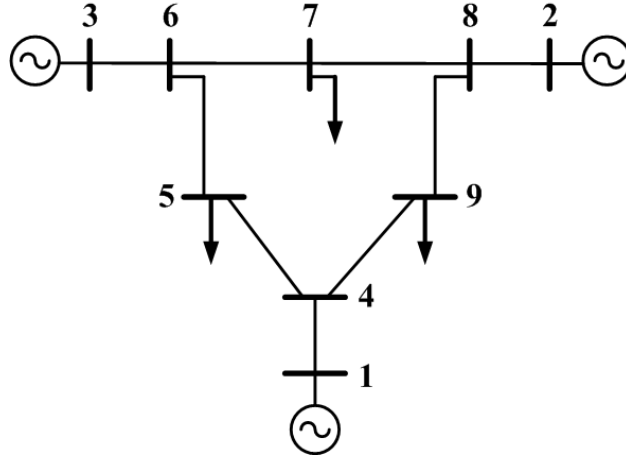


Figure 1: IEEE 9 Bus System

Since multiple distribution systems are identical in parallel, they are combined into one system, with impedance divided and P and Q values multiplied by several buses. This was done after comparing the results of this system with the original system and observing the same results.

7 CPF

7.1 Literature review

Continuation Power Flow (CPF) is a widely adopted technique for studying voltage stability in power systems under increasing load or generation. It provides a detailed analysis of the system's loadability limit or the maximum load that can be applied to the network before voltage instability occurs. Unlike traditional power flow methods, CPF introduces a load-scaling parameter, λ , which incrementally increases system

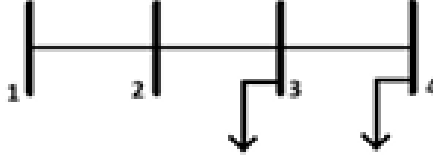


Figure 2: IEEE 4 Bus System

load in a controlled manner, enabling a smooth tracing of the power-voltage curve even beyond the point of voltage collapse.

The CPF method employs a **predictor-corrector approach**, which ensures both robustness and accuracy in tracking voltage changes. The predictor step estimates changes in system voltage and load for a given increment of λ , typically using a tangent vector derived from the Jacobian matrix of the system. This step enables CPF to predict system behavior beyond critical points where conventional methods fail due to singular Jacobian matrices. The **corrector step** then applies the Newton-Raphson Load Flow (NRLF) method to refine the predicted values, ensuring that the system's power flow equations remain balanced at each iteration.

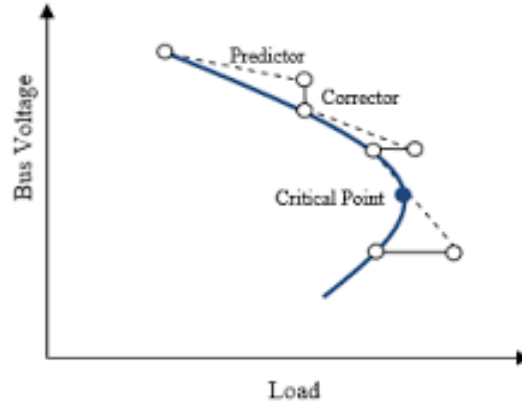


Figure 3: CPF

CPF operates in three phases:

1. Phase 1: Increases the load step by step, allowing the system to find stable voltage solutions.
2. Phase 2: Approaches the maximum load transfer point, where voltage stability becomes more critical.
3. Phase 3: Analyze the system near or beyond the voltage collapse point.

7.2 Methodology

The code for CPF was written in a Python function named 'runCPF' that implements a Continuation Power Flow (CPF) analysis.

Here's a breakdown of the code:

- **Input:**

1. **casedata**: Contains data about the power system (bus, branch, generator, etc.).
2. **BusForCPF**: Specifies the bus at which we are interested in tracking voltage changes.

- **Other Parameters:**

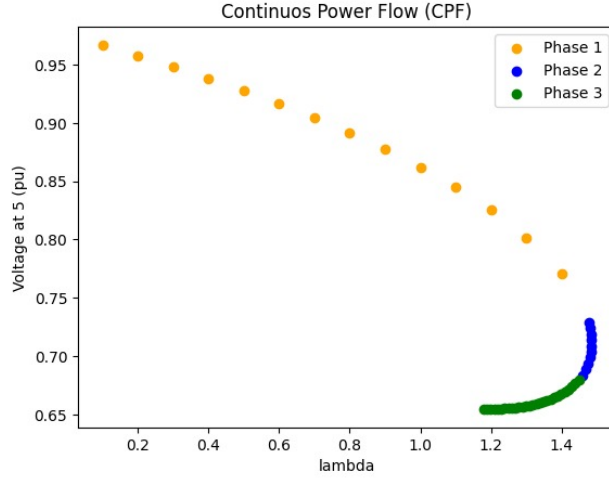


Figure 4: Different Phases in CPF at bus 5

1. **‘step1’, ‘step2’, ‘step3’:** Step sizes for the three phases of CPF.
2. **tolerance:** Convergence tolerance for the Newton-Raphson method.
3. **maxiterations:** Maximum number of iterations allowed for convergence.
4. **change factor:** Factor used to modify how lambda evolves during the analysis.

Main Steps in the Function:

- **Extracting and Preprocessing Data :**

1. BusData, BranchData, GenData, and basePower are extracted from casedata. These contain essential information about the system’s buses, branches, and generators.
2. The powers in BusData and GenData are converted to per unit (pu) by dividing them by the base power.
3. Voltage angles in BusData and BranchData are converted from degrees to radians.

- **Admittance Matrix Calculation (Ybus):**

1. Ybus is calculated using the function CalculateYbus. This matrix describes the relationships between voltages and currents at different buses in the system.

- **Bus Classification and Flat Start:**

1. Buses are classified into three types slack bus, PV Bus, and PQ Bus. The buses are then reordered for processing.
2. Flat Start: The initial voltage magnitudes (‘V’) are set to 1, and the voltage angles (‘d’) are set to 0. Voltages for the slack and PV buses are updated from the generator data.

- **Initial Power Scheduling (‘Psch’, ‘Qsch’):**

1. Active (‘Psch’) and reactive (‘Qsch’) power schedules are initialized for each bus. For buses with generators, the scheduled values are updated

- **Phases of CPF:** The CPF analysis is done in three phases, and each phase adjusts the power demand and the system’s response iteratively:

1. **Phase 1: Changing Lambda**

This phase focuses on changing the load factor (‘lambdaval’) and monitoring the response of the system.

The tangent vector is calculated using the Jacobian matrix, which provides the direction of movement for the system’s state variables (voltage angles, magnitudes) and ‘lambdaval’.

The system undergoes a predictor-corrector process where the state is predicted and then corrected using a Newton-Raphson Load Flow (NRLF) algorithm.

If the Jacobian matrix becomes singular, then the phase stops.

2. Phase 2: Modified Lambda

This phase starts from the last stable point in Phase 1 and then, a predictor-corrector approach is used, but the focus is on avoiding the collapse of ‘ λ_{bd} ’.

The correction step ensures that voltages and the system state converge within the specified tolerance.

The system exits this phase when no further significant progress can be made.

3. Phase 3: Final Stage

The third phase focuses on increasing ‘ λ_{bd} ’ as much as possible before reaching system limits.

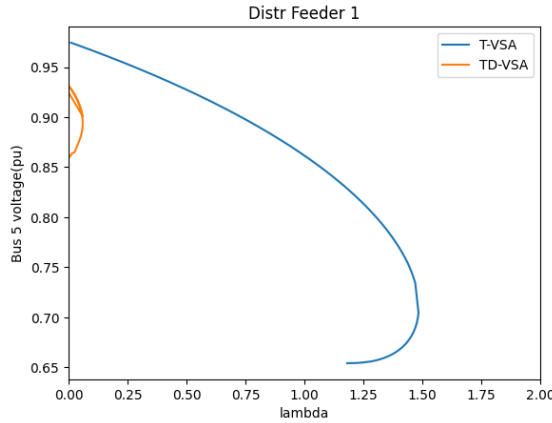
Similar predictor-corrector steps are performed, but with smaller step sizes to fine-tune the system’s behavior near its collapse point.

- **Outputs:** The function returns three things:

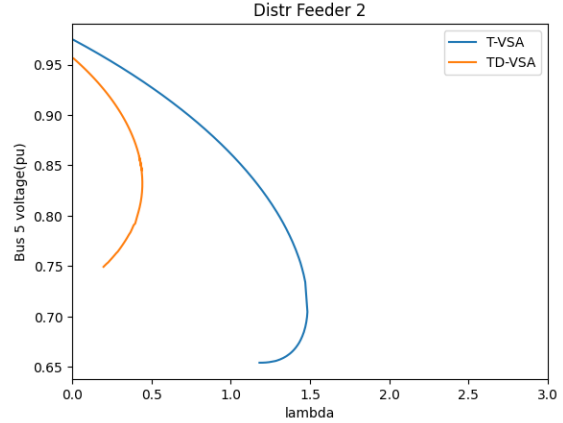
1. **XLambda:** A list of lambda values, which represent the load factor as the analysis progresses.
2. **YV:** A list of voltage magnitudes at the specified bus (‘BusForCPF’) for each value of lambda.
3. **JList:** The list of Jacobian matrices that provide insights into the system’s stability and sensitivity at each step.

7.2.1 Results of CPF

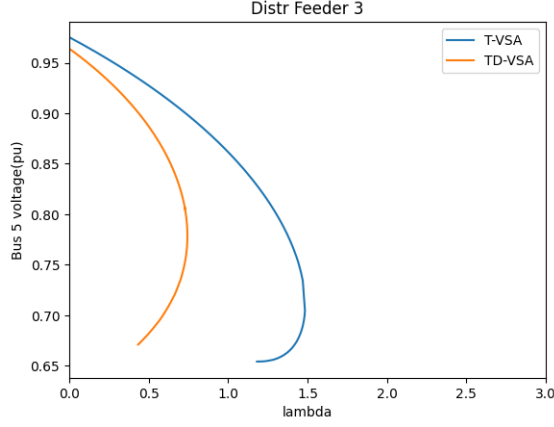
CPF was conducted on Bus 5 where different **Distribution systems** were connected. Below are the graphs showing the CPF of the Transmission system and the Transmission-Distribution system.



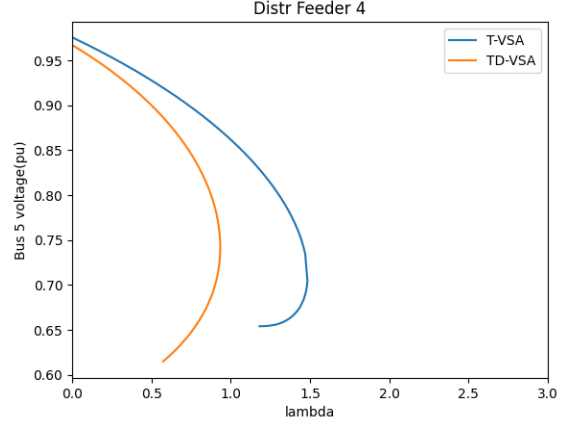
(a) $d1\text{correctionfactor} = 1$



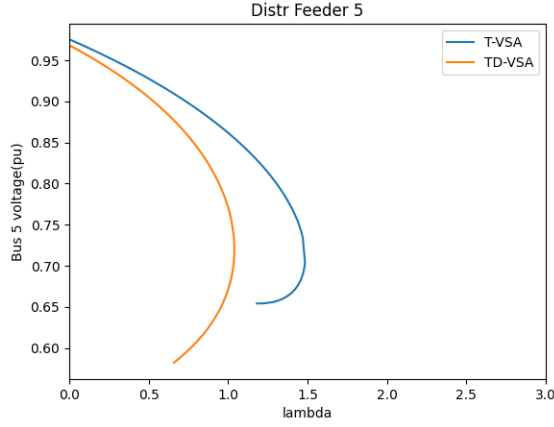
(b) $d1\text{correctionfactor} = 2$



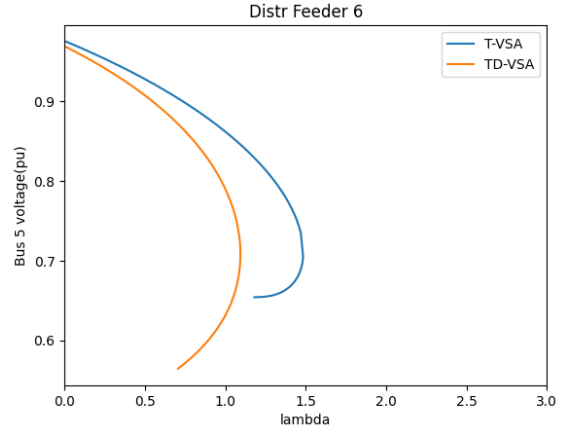
(a) $d1correctionfactor = 4$



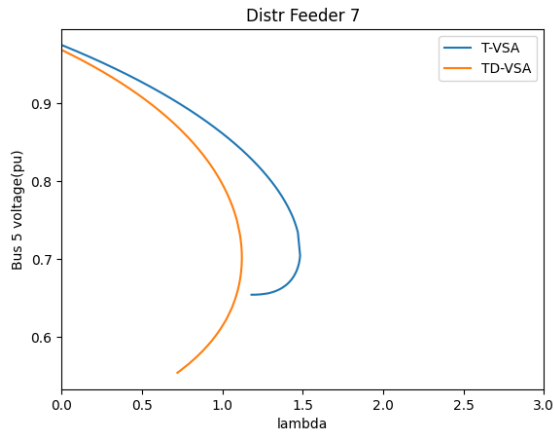
(b) $d1correctionfactor = 8$



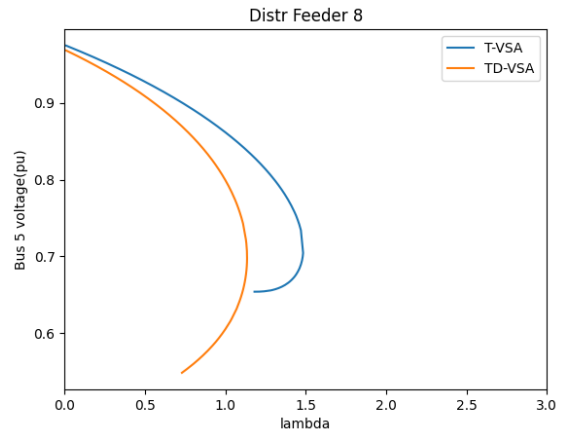
(a) $d1correctionfactor = 16$



(b) $d1correctionfactor = 32$



(a) $d1correctionfactor = 64$



(b) $d1correctionfactor = 128$

7.2.2 Inference

The CPF results for Transmission-only (T-VSA) and integrated Transmission-Distribution (TD-VSA) systems demonstrated that their P-V curves do not overlap, highlighting the limitations of T-VSA in capturing the interactions between transmission and distribution systems. When the distribution impedance (Z_{distr}) was reduced by a factor of 2, the difference in critical λ values decreased, indicating stronger coupling and

more aligned stability characteristics between the two systems. These findings emphasize the necessity of integrated TD-VSA for accurate voltage stability analysis, as T-VSA alone cannot account for the impact of distribution systems on overall system behavior.

7.3 Lumped Distribution System

In many voltage stability studies, especially when the focus is primarily on the transmission system, the entire distribution system is often represented as an equivalent (lumped) load connected at a single bus (usually the substation). However, a naive aggregation of only the real and reactive power can lead to significant errors in evaluating the actual loadability limits and voltage behavior. This is because the distribution system contributes not just to the power demand but also introduces voltage-dependent characteristics and losses, which impact the net power drawn from the grid.

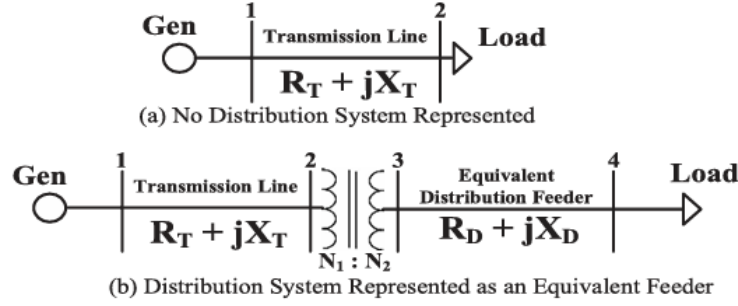


Figure 9: Equivalent system with and without distribution system

7.3.1 Methodology

To approximate the effect of a detailed distribution system within a transmission system stability analysis, we implemented a methodology to lump the distribution network into an equivalent load and impedance connected at the substation bus. This approach helps reduce system complexity while retaining the critical effects of voltage drops and losses typically seen in detailed TD-VSA studies.

We began by running a power flow (PF) analysis on the standalone IEEE 4-bus distribution system using the Newton-Raphson method. This was done to compute the net power drawn from the substation and the total power consumed across all loads. The difference between these two quantities gave us the real and reactive power losses in the distribution system.

- Substation power ($S_{sub} = P_{sub} + jQ_{sub}$): Net power flowing into the distribution system from the transmission grid.
- Total load power ($S_{load} = P_{load} + jQ_{load}$): Sum of all downstream loads.
- Total load power ($S_{load} = P_{load} + jQ_{load}$): Sum of all downstream loads.

7.3.2 Derivation

- Substation Current Magnitude:
The current injected into the distribution system is:

$$I_{sub} = \frac{S_{sub}^*}{V_{sub}}, \quad (1)$$

where V_{sub} is the substation voltage (obtained from PF results)

- Loss-Based Impedance:
The equivalent impedance is calculated by equating the losses to $I^2 Z$:

$$S_{loss} = P_{loss} + jQ_{loss} = |I_{sub}|^2 (R_{eq} + jX_{eq}). \quad (2)$$

Solving for R_{eq} and X_{eq} :

$$R_{eq} = \frac{P_{loss}}{|I_{sub}|^2}, \quad (3)$$

$$X_{eq} = \frac{Q_{loss}}{|I_{sub}|^2}. \quad (4)$$

- Per-Unit Conversion:

Convert R_{eq} and X_{eq} to per-unit values using the transmission system base (S_{base} , V_{base}):

$$R_{eq}^{pu} = \frac{R_{eq}}{Z_{base}} = \frac{R_{eq} \cdot S_{base}}{V_{base}^2}, \quad (5)$$

$$X_{eq}^{pu} = \frac{X_{eq}}{Z_{base}} = \frac{X_{eq} \cdot S_{base}}{V_{base}^2}. \quad (6)$$

To improve accuracy, Task 3 of the referenced methodology introduces a more rigorous approach to lumping by computing an equivalent complex power and impedance, denoted as S_ROM (Real-Only Model) and Z_ROM. This method involves:

1. Solving a full nonlinear power flow of the distribution system, considering all its loads, line impedances, and topology.
2. Calculating the net complex power injected at the boundary bus (i.e., the substation) by the distribution system.
3. Deriving an equivalent impedance using the relation

$$Z_{ROM} = \frac{V^2}{S_{ROM}^*}$$

where V is the substation voltage and S_{ROM} is the conjugate of the power drawn.

4. Replacing the full distribution system in the integrated model with a single equivalent load (Z_ROM) and injecting the total power demand (S_ROM) into the transmission system at the corresponding bus.
5. ZIP Model Integration: Instead of representing the distribution load as a constant power (P) load, incorporate a ZIP model where:
 - Z represents a voltage-dependent (quadratic) load
 - I captures linear dependency
 - P is the constant power term

This ensures a realistic approximation of how load demand varies with voltage.

This lumped equivalent was then used for continuation power flow (CPF) analysis and compared against the full TD-VSA model to assess how accurately the reduced-order representation mimicked the detailed system.

7.3.3 Results

- Orange Curve (T-VSA): This shows the loadability curve when the transmission system is analyzed independently, assuming distribution load is lumped as constant power at the substation (bus 5). It ignores the actual voltage drop and losses across the distribution system. Hence, it overestimates the voltage stability margin (VSM), showing a higher critical λ .
- Green Curve (TD-VSA): This represents the actual transmission-distribution (TD) system where the distribution network is explicitly modeled. Due to the presence of distribution losses and voltage drops, the substation voltage is lower, causing instability at a smaller value of λ .

- Blue Curve (TD-lumped): This curve is obtained by mimicking the detailed distribution feeder using a lumped impedance (R , X) and load (S_{ROM}) connected to the transmission substation. It shows lower voltage due to the drop across $R + jX$, resulting in a reduced λ limit. However, the curve begins at a very low voltage, indicating the chosen parameters may be too aggressive, leading to early voltage collapse.

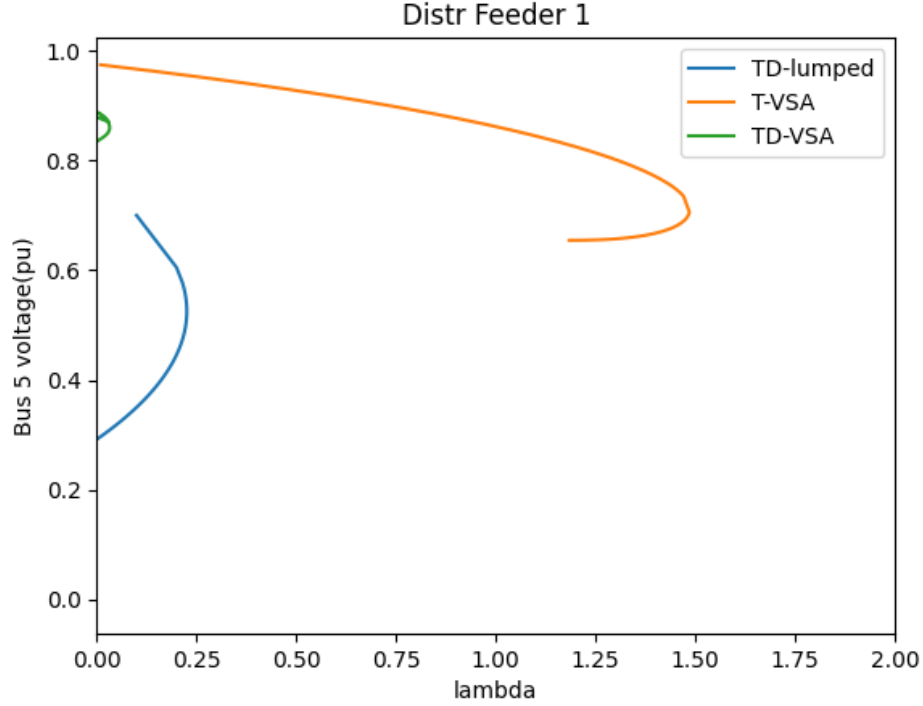


Figure 10: Comparison of λ -V curves for T-VSA, TD-VSA, and TD-lumped methods

7.3.4 Inferences

To simplify the integrated transmission-distribution system while retaining critical characteristics, the distribution network was replaced by an equivalent load and impedance ($R + jX$) attached to the transmission substation. This reduced-order model was derived using power flow analysis to estimate total substation power and distribution losses, from which the impedance was calculated. The ZIP model was also considered to reflect voltage dependency.

The λ -V graph compares three cases: T-VSA (transmission only), TD-VSA (full transmission-distribution system), and TD-lumped (transmission with equivalent distribution model). As expected, T-VSA showed the highest voltage stability margin (VSM), overestimating system capability by ignoring distribution effects. TD-VSA reflected the actual lower voltage at the substation due to real power losses and voltage drops in the distribution feeder. The TD-lumped curve, while simpler, approximated this behavior by introducing an impedance that captured distribution losses.

This method proves valuable in scenarios where detailed modeling is computationally expensive or unavailable. It helps capture critical stability behavior using minimal data, highlighting the importance of accurately representing the distribution network even in simplified power system studies. However, the results also emphasize the need to carefully tune equivalent parameters to avoid under- or overestimating the system's stability limits.

7.4 Addition of Renewable Energy Source

With the increasing penetration of Renewable Energy Sources (RES) such as solar and wind in modern power systems, their impact on voltage stability cannot be overlooked. Unlike traditional synchronous generators, RES are typically connected through power electronics and lack inherent voltage support capabilities unless properly controlled. Their intermittent nature also causes variability in power injection, which directly

influences the voltage profile of both distribution and transmission systems. Moreover, RES can provide or absorb reactive power under certain control schemes, significantly altering the load flow and voltage stability margins. Therefore, considering RES in integrated Transmission-Distribution Voltage Stability Assessment (TD-VSA) is crucial for realistic modeling, better planning, and enhanced system reliability under dynamic operating conditions.

7.4.1 Different Cases

- Comparison of Transmission system with and without RES
Added a RES of power (10MW, 10MW) to bus 4 of the transmission system.

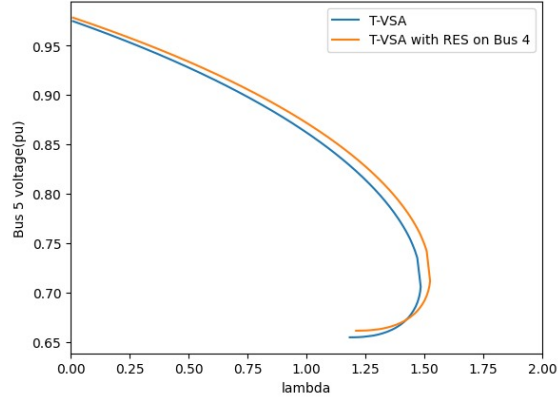


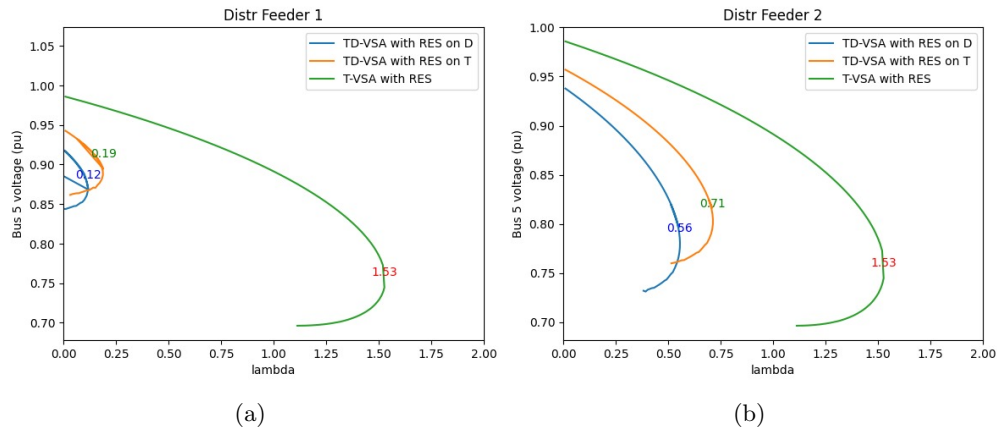
Figure 11: CPF plot: Effect of RES addition on Transmission system

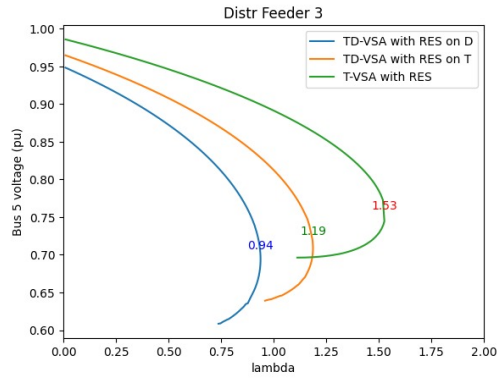
This plot illustrates the difference in voltage profiles with and without Renewable Energy Sources at bus 4:

1. Blue Curve (Without RES) shows a steeper voltage drop as the load increases, leading to an earlier voltage collapse (lower λ)
2. Green Curve (With RES) maintains higher voltage levels for the same load growth, reflecting the local support provided by DER, which delays the onset of instability

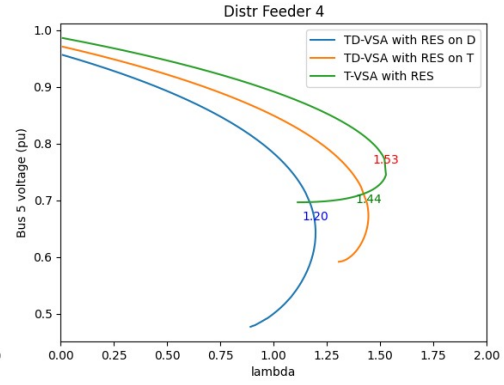
The plot confirms that RESs enhance voltage stability and increase the loadability margin of the system

- Comparison of TD system with and without RES
Added a RES of power (10MW, 10MW) to bus 2 of distribution bus. We get the following 8 graphs of 8 different feeders where with every increase in feeder number the impedances are reducing by a factor of 2.

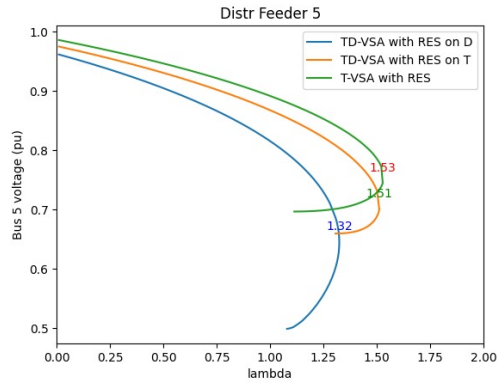




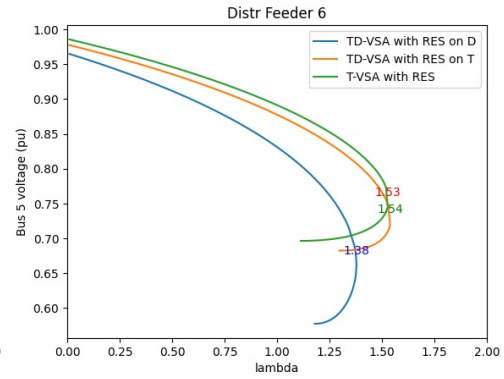
(a)



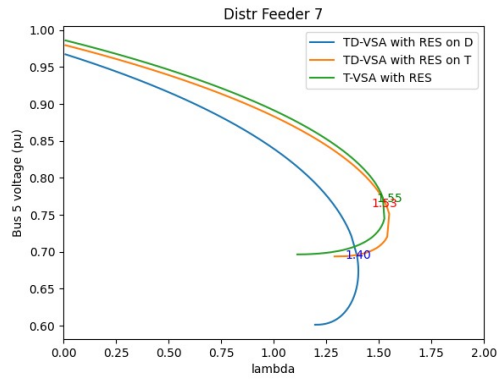
(b)



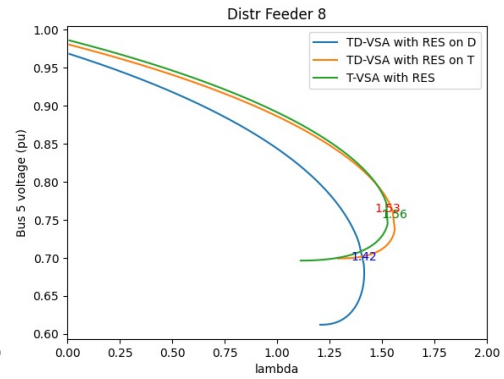
(a)



(b)



(a)



(b)

To analyze the effect of Distributed Energy Resources (DERs) on voltage stability, different scenarios were studied using different distribution feeder configurations. Each scenario compares the following three voltage stability assessments:

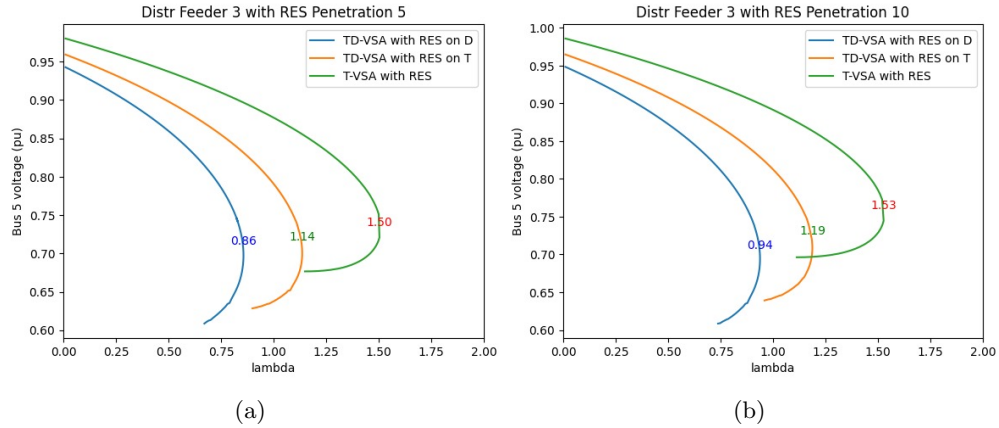
- T-VSA with RES (Green Curve): Transmission-only system with an equivalent load of (80 MW + 20 MW) modeled at Bus 5. DER effects are aggregated without modeling distribution topology.
- TD-VSA with RES on T (Orange Curve): Full Transmission-Distribution (TD) system, where the entire 20 MW of DER is placed at the transmission level (Bus 4).
- TD-VSA with RES on D (Blue Curve): Full TD system, but DER (1 MW) is placed at Bus 2 within the distribution network. The impact of DER placement location is explicitly modeled.

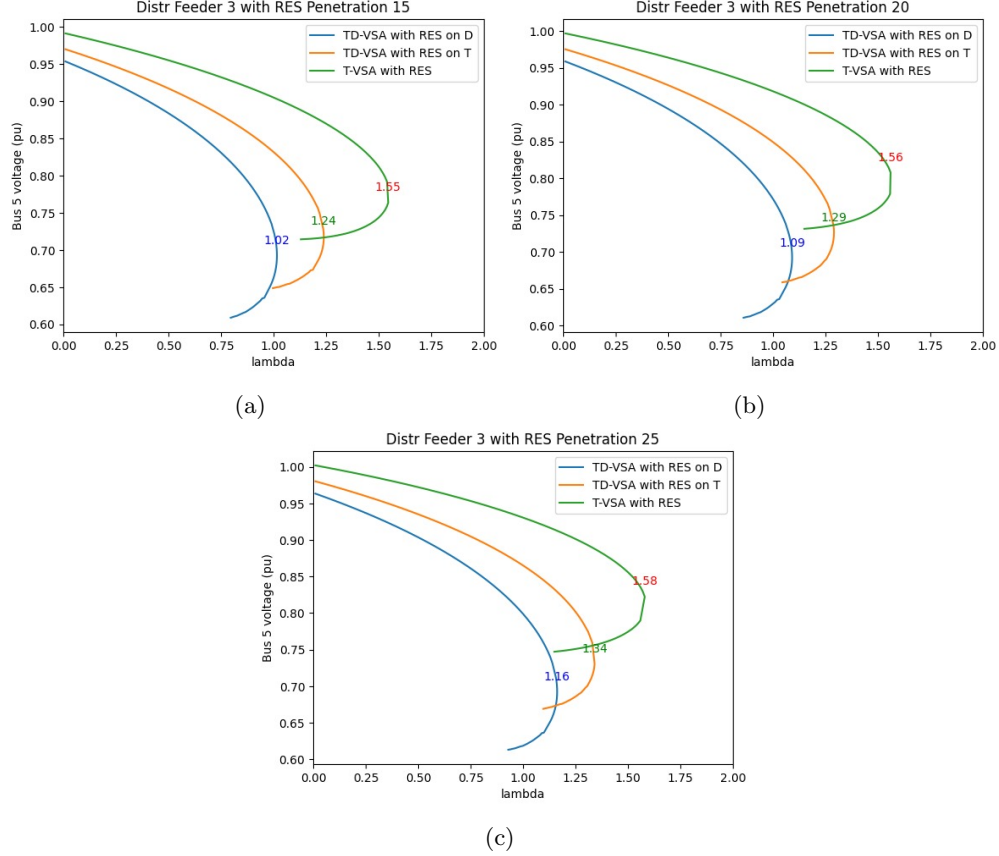
Feeder No.	TD,RES on D Max	TD,RES on T Max	T,RES Max	% Change
1	0.1200	0.1900	1.5270	-36.84%
2	0.5563	0.7134	1.5270	-22.02%
3	0.9378	1.1872	1.5270	-21.01%
4	1.1965	1.4445	1.5270	-17.16%
5	1.3234	1.5110	1.5270	-12.41%
6	1.3780	1.5388	1.5270	-10.45%
7	1.4032	1.5500	1.5270	-9.47%
8	1.4155	1.5611	1.5270	-9.33%
9	1.4215	1.5600	1.5270	-8.88%

Table 1: Maximum Loadability Comparison across Feeders

This table presents the maximum loadability values for each feeder for the different cases discussed, along with the percentage change in loadability between TD with RES on T and TD with RES on D systems.

- RES Penetration : Now, we have increased the RES penetration power starting from (5MW, 5MW) to (25MW, 25MW). This is done on distribution feeder 3.





RES Penetration	TD,RES on D Max	TD,RES on T Max	T,RES Max	% Change
5	0.8568	1.1361	1.5035	-24.59%
10	0.9378	1.1872	1.5270	-21.01%
15	1.0159	1.2388	1.5453	-17.99%
20	1.0908	1.2903	1.5600	-15.46%
25	1.1625	1.3410	1.5800	-13.31%

Table 2: Maximum Loadability Comparison for Different RES Penetrations

Increasing RES penetration clearly improves the VSM, reinforcing the grid's ability to handle more load before instability.

7.4.2 Inferences

The integration of Renewable Energy Sources (RES) into the power system, particularly at the distribution level, introduces both opportunities and challenges for voltage stability. In our study, RES were modeled as negative loads (i.e., power injections), and we examined their effect on the voltage stability margin (VSM) using continuation power flow (CPF) across different scenarios. By strategically placing RES either at the transmission bus or within the distribution feeders, we observed how the location of generation significantly alters system behavior.

When RES is added at the transmission level, it offsets the load seen by the transmission system, resulting in a moderate improvement in VSM. However, placing RES within the distribution network reveals more nuanced effects. If RES is located far from the substation (deep in the feeder), it can cause localized voltage rise and reverse power flows, which paradoxically lead to reduced VSM and earlier voltage collapse. In contrast, RES placed closer to the substation provides better voltage support and more effectively improves overall system stability.

The results highlight that merely considering the total power from RESs is insufficient. Accurate modeling of their location within the network is crucial. This underscores the importance of coordinated Transmission-Distribution Voltage Stability Assessment (TD-VSA) for planning and operating power systems with in-

creasing RES penetration.

8 Jacobian Determinant Analysis

For the 4 bus distribution system in connection as shown above in figure2, the system has the following buses:

1. Bus 2,3 are PV buses, and bus 4-9 are PQ buses, of the transmission system.
2. Thus for bus 2-9, the Active power value is specified, and for bus 4-9, the reactive power value is specified.
3. Bus 10-13 are PQ buses of the distribution system.
4. The distribution system and transmission system are connected only by bus 5-bus 10 branch

	P						Q							
Bus	2	...	9	10	11	...	13	4	...	9	10	11	...	13
2	T				0			T				0		
⋮														
9														
10														
11	0				D			0				D		
⋮														
13														
4	T				0			T				0		
⋮														
9														
10														
11	0				D			0				D		
⋮														
13														

Figure 18: General Form of Jacobian

So many entries are 0 because there is no direct connection between those buses. As interchanging rows and columns do not change the magnitude of the determinant of the Jacobian (which is considered a measure of closeness to the collapse point), so rearranging the Jacobian by interchanging rows and columns gives this form:

In the above Jacobian, the T and D submatrices can be considered to represent Transmission and distribution-only systems. In further analysis, the Jacobian is divided into T and D parts based on these criteria. Note that bus 10 is not considered in any of the two parts, and is taken as a combined extra bus.

8.1 Determinant of Jacobian using CPF

The code for calculating CPF was executed, and at the end of each iteration, the converged Jacobian was stored. This generated a list of converged Jacobian matrices. Each matrix in this list was split into transmission and distribution sub-matrices and the determinant of each sub-matrix. This generated the below plot:

Bus	2	...	9	4	...	9	10	10	11	...	13	11	...	13
2	T								0					
⋮														
9														
4														
⋮														
9														
10														
10														
11	0								D					
⋮														
13														
11														
⋮														
13														

Figure 19: Rearranged Form of Jacobian

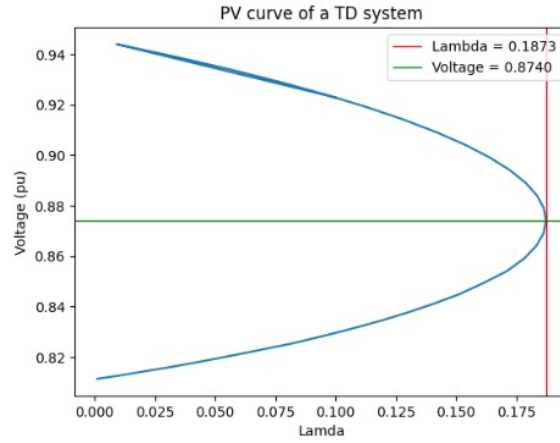
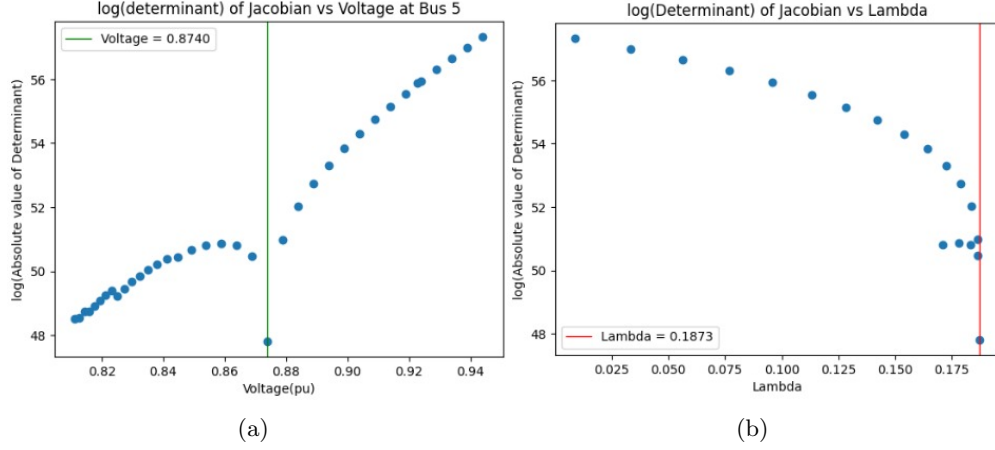


Figure 20: CPF plot: V at max loadability=0.874

- In CPF, the voltage at bus 5 corresponding to maximum loadability is 0.874. The dip in the determinant of a total Jacobian matrix is also visible at a voltage of 0.87. This verifies the fact that, near loadability limit, the Jacobian determinant tends towards 0.
- The trend that the determinant of the D sub matrix tends to 0 at some other voltage was not investigated further.
- The determinant of the total matrix was not becoming very small, as the step size was relatively large to observe that pattern. It was tried to get this by iterative analysis, present in the next sub-section.

The graph illustrates the relationship between the logarithm of the absolute value of the Jacobian determinant and the voltage at Bus 5, analyzed through CPF. A notable dip in the determinant's value is observed near the voltage of 0.874 pu, which corresponds to the maximum loadability point, confirming that the Jacobian determinant approaches zero near the loadability limit. This validates the theoretical expectation that system stability diminishes at critical points. However, the determinant of the distribution sub-matrix (D-matrix) trends towards zero at a different voltage, a phenomenon not explored further. Additionally, the determinant of the total Jacobian matrix did not approach zero as sharply due to the relatively large step size in CPF, which limited finer observations.



9 Voltage Stability Index (VSI)

9.1 Introduction

The VSI provides a measure of the voltage stability margin at each bus. It is calculated using the Thevenin equivalent impedance (Z_{th}) and the load impedance (Z_{load}) at each bus:

$$VSI = \frac{Z_{th}}{Z_{load}}$$

It helps in identifying weak buses or regions in the grid that are prone to voltage collapse, which is critical for system planning and operation.

A VSI value approaching 1 signals that the bus is nearing its voltage instability limit, indicating that further load increases (represented by higher lambda values) could lead to system collapse. Conversely, lower VSI values reflect a greater stability margin, signifying better voltage stability at the bus.

9.2 Methodology

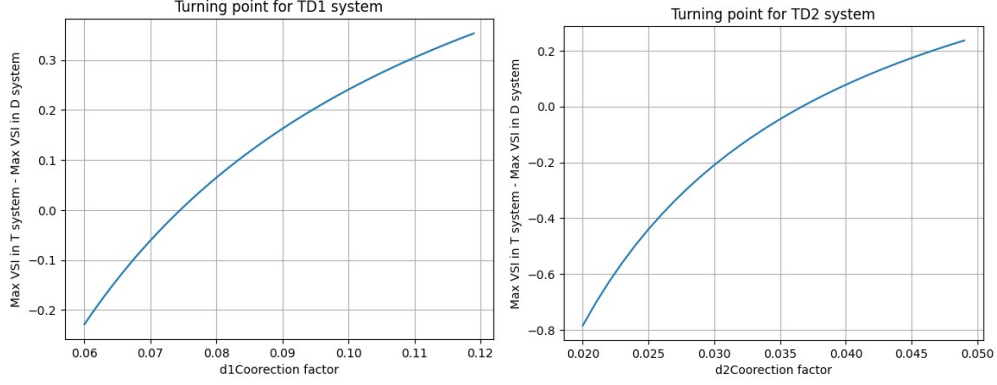
VSI is calculated for a bus at a lambda value.

1. **Zload:** represents how much the connected devices resist the flow of electric current. It is determined by the active power (P) and reactive power (Q) that the load is consuming. The voltage at the bus where the load is connected and the changes in the power demand (represented by lambda). If there is no power consumption, Zload becomes infinitely high because there is nothing resisting the flow of electricity.

$$Z_{load} = \frac{V^2}{S}$$

where $S = P + jQ$

2. **Zthev:** represents the internal resistance of the network seen from a specific bus. To calculate Zthev we used two different methods: Kron's Reduction and Zbus Matrix.
 - **Method 1 - Kron's Reduction:** The power system can be represented as the Ybus matrix. We can derive the Thevenin impedance using mathematical transformations by reordering the Ybus matrix and isolating the bus of interest. However, this method sometimes gives inaccurate results because it assumes the system behaves in a simplified way.
 - **Method 2 - Zbus matrix:** Instead of reducing the network, this method constructs a matrix called Zbus, which directly gives the Thevenin impedance for each bus. The Zbus matrix is built by considering all the electrical connections (branches) and how they interact. The diagonal elements of the Zbus matrix give us the Thevenin impedance for each bus, making it a more reliable approach.



(a) VSI = 0 at d1correctionfactor = 0.074 (b) VSI = 0 at d2correctionfactor = 0.0364

9.3 Results

VSI for all the buses of the TD System was calculated. Below are the graphs:

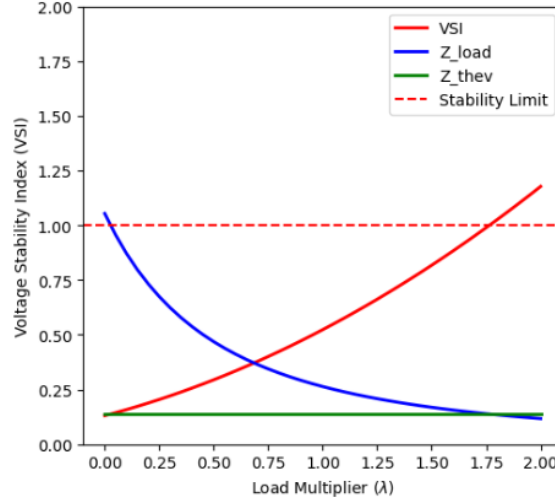


Figure 23: VSI values for increasing lambda

The above plot shows the values of VSI, Zload, and Zthev at Bus 5 for increasing lambda value. We are getting VSI = 1 at lambda = 1.76, which is the loadability limit for stability, whereas in CPF Analysis, we got lambda = 1.48 as the loadability limit.

9.4 Inference

The Voltage Stability Index (VSI) for all buses in the Transmission-Distribution (TD) system was analyzed under varying correction factors. Initially, with $d1$ and $d2$ correction factors set to 1, the VSI calculation showed that bus 9 in the transmission system had the highest value, indicating it was the most stable (VSI = 0.91). The correction factors were reduced to investigate how instability might shift between the transmission and distribution systems. The difference between the maximum VSI values in the transmission (T) and distribution (D) systems was then plotted. The results revealed that for smaller correction factors, the VSI of the distribution system exceeded that of the transmission system (the difference was negative). At $d1\text{correctionfactor} = 0.074$ and $d2\text{correctionfactor} = 0.0365$, the VSI values for T and D systems were equal, suggesting a balanced instability point. Beyond these values, the difference became positive, indicating that the instability would primarily originate from transmission buses rather than distribution buses. This analysis highlights how changes in distribution parameters influence the voltage stability dynamics across the integrated system.

10 Transmission Distribution Distinguishing Index

10.1 Introduction

The Transmission-Distribution Distinguishing Index (TDDI) is a numerical value used in power systems to identify whether voltage stability limits in an electrical grid are mainly caused by the transmission network (high-voltage side) or the distribution network (low-voltage side).

It is calculated using the impedances of the transmission and distribution systems, represented as Z_T and Z_D . The TDDI formula is:

$$\text{TDDI} = \log \left(\frac{Z_T}{Z_D} \right)$$

1. Positive TDDI: The transmission network is the limiting factor (transmission-limited).
2. Negative TDDI: The distribution network is the limiting factor (distribution-limited).
3. TDDI = 0: Both networks are equally contributing to the voltage stability limit.

TDDI helps power system operators quickly identify whether to fix issues on the high-voltage side or the low-voltage side, ensuring a targeted and efficient response to maintain grid stability.

10.2 Result

TDDI when calculated for `d1correctionfactor = 1` and `d2correctionfactor = 1` resulted in **-2.485** indicating that the Distribution system is the limiting factor.

11 Bus Participation Factor

This analysis focuses on **Bus Participation Factors (BPF)**, **Voltage-Current (V-Q) Sensitivity**, and their relationship in identifying **critical modes** and ensuring system stability.

11.1 V-Q sensitivity Analysis

The V-Q sensitivity at a bus represents the slope of Q-V curve at the given operating point. A positive V-Q is indicative of stable operation; the smaller the sensitivity, the more stable the system. As stability decreases the magnitude of sensitivity increases, becoming infinite at the stability limit. Conversely, a negative V-Q sensitivity is indicative of unstable operation. A small negative sensitivity represents a very unstable operation. The relationship between active power (ΔP) and reactive power (ΔQ) can be expressed using the Jacobian matrix (J):

$$\begin{bmatrix} \Delta P \\ \Delta Q \end{bmatrix} = \begin{bmatrix} J_{P\theta} & J_{PV} \\ J_{Q\theta} & J_{QV} \end{bmatrix} \begin{bmatrix} \Delta \theta \\ \Delta V \end{bmatrix}.$$

By keeping active power constant ($\Delta P = 0$), the relationship simplifies to:

$$\Delta Q = J_R \Delta V,$$

where J_R is the reduced Jacobian matrix:

$$J_R = J_{QV} - J_{Q\theta} J_{P\theta}^{-1} J_{PV}.$$

J_R is central for analyzing **V-Q sensitivity** and **stability margins**. Eigenvalues and eigenvectors derived from J_R provide insight into **critical modes** and system stability.

- *+ve* slope: Stable operation.
- *-ve* slope: Unstable operation.

The sensitivity relationship is given by:

$$\Delta V = J_R^{-1} \Delta Q,$$

Eigenvalue Decomposition of J_R :

$$J_R^{-1} = \xi \Lambda^{-1} \eta,$$

where:

- ξ : Right eigenvector matrix of J_R ,
- η : Left eigenvector matrix of J_R ,
- Λ : Diagonal eigenvalue matrix.

This allows:

$$\Delta V = \sum_i \frac{\xi_i \eta_i}{\lambda_i} \Delta Q.$$

Sensitivity Expression: For a specific bus k :

$$\frac{\partial V_k}{\partial Q_k} = \sum_i \frac{\xi_{ki} \eta_{ik}}{\lambda_i}.$$

Eigenvalues (λ_i) close to zero indicate **critical modes**, where small changes in Q can cause large variations in V , signaling instability.

11.2 Modes

Definition: Modes represent the dynamic behavior of the power system, typically the eigenvalues of the reduced Jacobian (J_R):

- **Stable modes:** Eigenvalues with negative real parts.
- **Unstable modes:** Eigenvalues with positive real parts.
- **Critical modes:** Eigenvalues near zero, indicating marginal stability.

V-Q Sensitivity Contribution: Critical modes correspond to eigenvalues that dominate the system's response, evaluated using **Bus Participation Factors (BPFs)**.

11.3 Bus Participation Factor

The Bus Participation Factor (BPF) is used in small-signal stability analysis to determine how much each bus contributes to a particular critical mode (eigenvalue) of the system. A high participation factor for a bus in a given mode means that the bus has a significant influence on that mode's dynamics. BPF_{ki} measures the participation of bus k in mode i . It reflects the relative influence of a specific bus on a particular eigenvalue (mode):

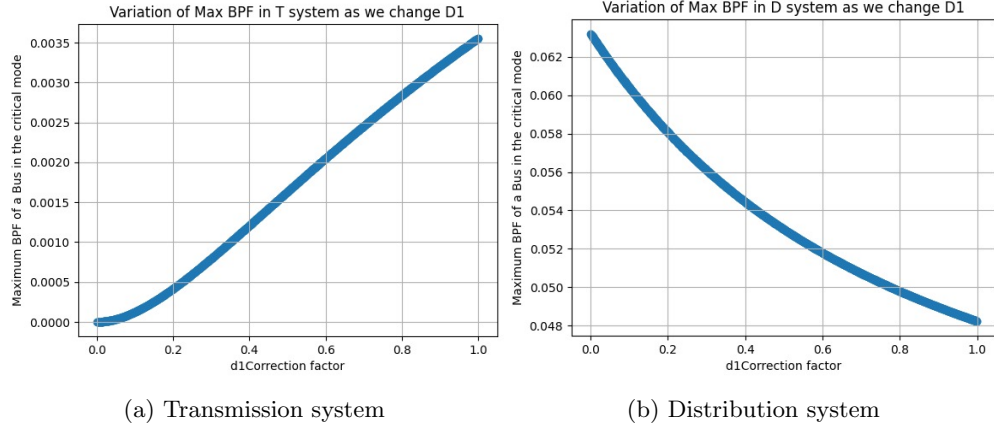
$$P_{ki} = \xi_{ki} \eta_{ik}.$$

A high P_{ki} value indicates that bus k strongly influences mode i . Such buses are critical to system stability.

System Description:

- Transmission System: 9 buses (1 slack, 2 PV, 6 PQ).
- Distribution System: 1 common bus, 10 radial systems (3 buses each).
- Total: 31 PQ buses + 6 PQ buses = **37 PQ buses**.

Critical Mode Identification: The least eigenvalue of J_R corresponds to the critical mode.



(a) Transmission system

(b) Distribution system

Here, we found the critical mode (least eigenvalue) and plotted the maximum value of BPF in the Transmission or Distribution system in that mode.

11.4 Conclusion

- **Modes and Stability:** The eigenvalues of J_R reveal the system's stability margins. Critical modes (eigenvalues near zero) signal instability.
- **BPFs:** Identify buses with the highest influence on these critical modes, helping to target corrective actions like reactive power support or capacitor placement.
- **Graphs:** Variations of maximum BPF with $D1$ correction factors highlight shifts in sensitivity between transmission and distribution systems.

12 References

1. A. K. Bharati and V. Ajjarapu, "Investigation of Relevant Distribution System Representation With DG for Voltage Stability Margin Assessment," *IEEE Transactions on Power Systems*, vol. 35, no. 3, pp. 2074-2083, May 2020, doi: 10.1109/TPWRS.2019.2950132.
2. Ajjarapu, V., and Christy, C. (1992). The continuation power flow: A tool for steady state voltage stability analysis. *IEEE Transactions on Power Systems*, 7(1), 416–423.
3. Ramapuram, A., Singhal, A., and Ajjarapu, V. (2019). Monitoring Long Term Voltage Instability due to Distribution and Transmission Interaction using Unbalanced muPMU and PMU Measurements. *IEEE Transactions on Smart Grid*.
4. Kundur, P. (1994). *Power System Stability and Control*. McGraw-Hill Education.
5. IEEE Xplore. (2019). Voltage Stability Analysis Using Hybrid Analytical and Numerical Continuation Methods. Retrieved from
6. Som, S. (2019). Continuation Power Flow. GitHub Repository. Retrieved from (<https://github.com/sayonsom/continuation-power-flow>).
7. ResearchGate. Diagram of the IEEE 9-bus test system. <https://www.researchgate.net/figure/Diagram-of-the-IEEE-9-bus-test-systemfig2303381482>
8. ResearchGate. An illustration of the IEEE 4-bus distribution system (<https://www.researchgate.net/figure/An-illustration-of-the-IEEE-4-bus-distribution-system-21fig4316351891>).